Surface-phonon polariton on gratings of GaP thin slabs: Far-infrared reflection

Jun-ichi Watanabe*
Institute of Physics, University of Tsukuba, Tsukuba-shi, Ibaraki 305, Japan

Kunimitsu Uchinokura
Department of Applied Physics, The University of Tokyo, 7-3-1 Hongo, Bunkyo-ku, Tokyo 113, Japan

Tomoyuki Sekine
Institute of Physics, University of Tsukuba, Tsukuba-shi, Ibaraki 305, Japan
(Received 13 December 1988; revised manuscript received 31 March 1989)

Surface-phonon polaritons on the gratings of GaP thin slabs are observed by far-infrared-reflectivity measurement without using an attenuated-total-reflection prism. The reflectivity spectra show a small dip at the frequency of the surface-phonon polariton. The experimental results are analyzed by extending the improved first-order perturbation theory of Yamashita and Tsuji [J. Phys. Soc. Jpn. **52**, 2264 (1983)] and are interpreted by the resonance effect between the surface-phonon polariton and the photon outside the sample. A small hump was observed in the reflectivity spectra near the frequency of the transverse-optical phonon with the formation of the grating. This was a new feature and interpreted also by the mixing of the photon with the surface-phonon polariton on the grating, as was in the case of the dip. It is not due to the resonance effect but is due to the back-scattering process via the creation of the surface-phonon polariton, which is associated with the divergent nature of the dielectric function. All of the features were consistent with the perturbation theory.

I. INTRODUCTION

The surface-phonon polariton is a coupled mode of the electromagnetic wave (photon) and an infrared-active optical phonon localized near the surface. On a flat interface between the air and a dielectric material, it has a dispersion relation in the region $\omega < ck_{\parallel}$, where ω is the frequency, c is the light velocity, and $k_{\parallel}$ is the wave vector parallel to the surface. It cannot have the corresponding photon mode outside the sample and is called the nonradiative mode. Usually, we can observe a nonradiative mode using the attenuated-total-reflection (ATR) method. Through the ATR prism with a large refractive index, the photon is given a wave vector $k_{\parallel}$ parallel to the surface large enough to be coupled to the nonradiative mode. Another method to observe a nonradiative mode is to rule a periodic structure (grating) on the surface. The nonradiative mode is given a $k_{\parallel}$ small enough ($\omega < ck_{\parallel}$) to be coupled to the photon outside the sample by the grating diffraction, i.e., the dispersion relation of the surface-phonon polariton is "folded" in the radiative region by the periodicity of the grating.

The surface polaritons are quite sensitive to the conditions of the surface. The surface roughness is one of the most important surface conditions. The ruled grating is a controlled surface roughness and a simple model of the surface roughness. In the present experiment, we shall show that the surface-phonon polaritons on the grating can be observed by the conventional far-infrared-reflectivity measurements without an ATR prism. The experimental results on the grating surface without the ATR prism can be more easily analyzed than those on the grating surface with the ATR prism. We shall provide the experimental results that the grating effect can be studied without the ATR prism for the surface-phonon polariton.

Although the surface-plasmon polariton on a grating is well investigated, little attention has been paid to the experimental and theoretical studies of the surface-phonon polariton on a periodic structure. The surface-phonon polariton has been observed only in periodically twinning planes of ZnSe thin film by means of conventional far-infrared-reflectivity (FIR) measurement.[1] In this paper we study experimentally the conventional FIR reflectivity of surface-phonon polariton on GaP grating and compare the experimental result with a theoretical reflectivity. A perturbation theory for the surface-plasmon polariton in a metal surface was adapted to the case of the surface-phonon polariton.

We also investigated Raman scattering of the surface-phonon polariton on the grating surface and shall report its results separately. A part of the present work has been reported briefly.[2]

II. EXPERIMENTAL DETAILS

A. Sample preparation

The grating structure is produced on $(\bar{1}\,\bar{1}\,\bar{1})$ surface (phosphorus face) of single-crystal GaP using a photolithographic technique described as follows. (1) A flat surface of GaP is prepared by mechanical polishing with diamond powder of 0.5 μm in diameter. (2) A thin film (thickness of about 0.3 μm) of SiO_2 is made using chemical-vapor-deposition method on the GaP surface. (3) The grating pattern is formed on the SiO_2 film by means of the photolithographic method. (4) GaP under the opening of the SiO_2 mask is etched by an aqueous solution of 0.5 mol KOH+1 mol $K_3Fe(CN)_6$ per liter. The grating pattern is formed on the GaP surface. (5) Finally, the SiO_2 mask is removed by an aqueous solution of ammonium fluoride.

The cross section of the grating was observed using a scanning electron microscope and was confirmed to have

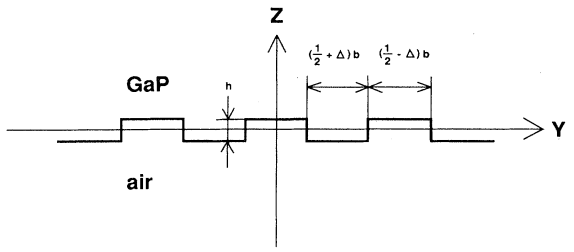

FIG. 1. Schematic structure of the grating.

an approximately square-wave profile as illustrated in Fig. 1. The average period of the grating b was 16.00 μm, and the average width of the groove was 7.86 μm which is slightly narrower than $b/2$. The groove depths h were about 0.2, 0.8, and 1.2 μm. The direction of the groove lines is $[\bar{1}\,\bar{1}\,2]$. The thickness of the samples was 0.1 mm.

The grating profile is described by the function

$$z=\xi(y)\ ,$$

$$\xi(y)=\begin{cases}(\frac{1}{2}+\Delta)h & \text{for } -\frac{1}{2}(\frac{1}{2}-\Delta)b<y<\frac{1}{2}(\frac{1}{2}-\Delta)b \\ -(\frac{1}{2}-\Delta)h & \text{for } \frac{1}{2}(\frac{1}{2}-\Delta)b<y<\frac{1}{2}(\frac{3}{2}+\Delta)b\ ,\end{cases} \tag{2.1}$$

$$\xi(y+b)=\xi(y)\ ,$$

where $\Delta=0.009$. Expanding it by Fourier series, we obtain

$$\xi(y)=\sum_{l=-\infty}^{\infty}\xi_{lg}\exp(ilgy),\quad g=2\pi/b\ , \tag{2.2}$$

where

$$\xi_{lg}=\begin{cases}\dfrac{h}{\pi l}\sin\pi l(\frac{1}{2}-\Delta) & \text{for } l\neq 0 \\ 0 \text{ for } l=0\ .\end{cases} \tag{2.3}$$

Fourier coefficients have the property

$$\xi_{lg}=\xi_{-lg}\ , \tag{2.4}$$

which comes from the fact that our grating has mirror symmetry with respect to the x-z plane (or $y=nb/2$ planes, where n is an integer). The opposite surface of the sample was flat.

B. FIR reflection

The reflectivity measurement was carried out in the FIR region (from 200 cm^{-1} to 600 cm^{-1}) by a Fourier-transform FIR spectrometer (Beckman IR-720M) at room temperature. The incident and reflected angles θ were $10\pm10°$. The incident and reflected beams were unpolarized. The instrumental width was about 2.5 cm^{-1}. An aluminum slab with optical flat surface was used as a reference mirror. The intensity of the interferrogram was digitally stored and was transformed by a fast-Fourier-transform program of a microcomputer. The direction of the incident light is perpendicular to the groove lines of the grating. The excitation of the surface polariton occurs only for the polarization of the light perpendicular to the grooves,[3] because the surface-phonon polariton is a p-polarized wave. The diffracted angle β of the mth (m is an integer) order diffracted light is given by

$$\sin\beta=m\lambda/b+\sin\theta\ , \tag{2.5}$$

where λ is the wavelength of the incident FIR light. The value of λ corresponding to the frequency of the surface-phonon polariton is about 25 μm in this experiment. Then we are led to the following condition:

$$|\sin\beta|>1 \quad \text{for } m\neq 0\ . \tag{2.6}$$

Equation (2.6) shows that there exists no diffracted light in the present condition. Under the condition of no diffracted light, we can efficiently observe the surface-phonon polariton without losing the intensity of the incident light to the diffracted light.

III. EXPERIMENTAL RESULTS

A reflectivity spectrum R_g of the grating surface of GaP is shown in Fig. 2(a). The thickness of the sample is about 0.1 mm, and the groove depth of the grating is 1.2 μm. The oscillations outside the reststrahlen band is the Fabry-Perot interference pattern of the GaP slab. In the reststrahlen band we see a small dip. For reference spectrum we measure the reflectivity R_f of the flat sample [see Fig. 2(b)]. The thickness of the sample was 0.5 mm so that the interference pattern could not be observed. To see the change of the reflectivity due to the grating we

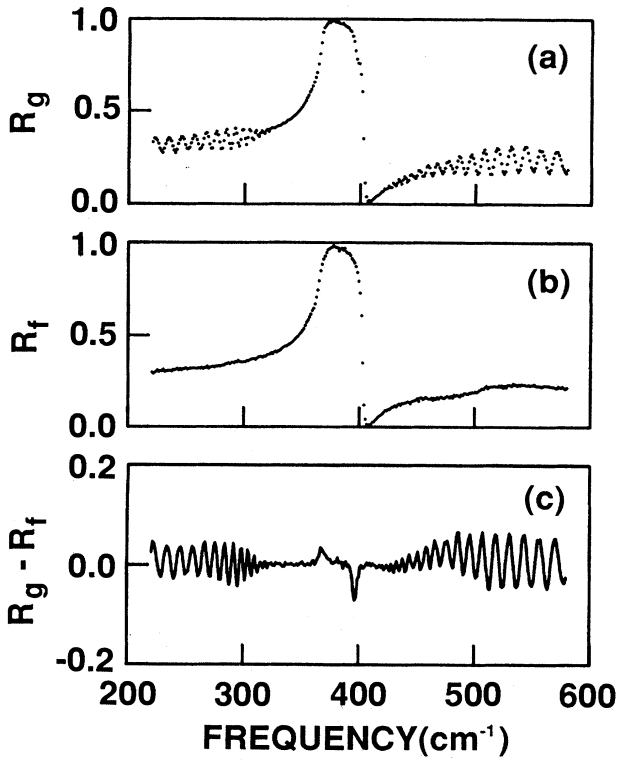

FIG. 2. The FIR reflectivity of the grating on the GaP surface (a), the flat surface (b), and the difference (c). The thicknesses of the samples with the grating and with the flat surface are 0.1 and 0.5 mm, respectively. The interference pattern is observed for the sample with the grating and is caused by the reflected FIR light on the front and back surfaces.

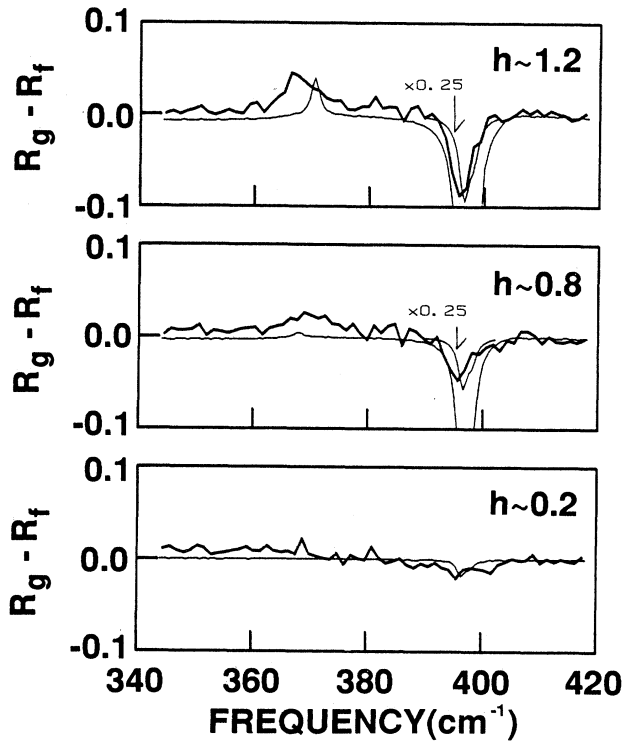

FIG. 3. The grating-groove-depth dependence of the FIR spectra obtained by subtracting the reflectivity of the flat surface from that of the grating on the GaP surface. Thick solid curve, experiment; and thin solid curve, calculation. The groove depth is indicated in each figure in μm.

show the difference $R_g - R_f$ between the reflectivities of the grating surface and the flat surface in Fig. 2(c). The difference spectrum clearly has a dip at about 396 cm^{-1}, which will be shown to come from the resonance between the photon outside the sample and the surface-phonon polariton on the grating. On the other hand, the most unexpected feature is the increase of the reflectivity near the frequency of the transverse-optical phonon ω_{TO}. The increase has never been observed before and will be also explained for the first time in this paper by the mixing of the photon with the surface-phonon polariton on the grating.

In Fig. 3 we show the dependence of the difference spectra on the groove depth. It is clear that the amplitude of the dip and the hump of the difference spectrum increase with the increase of the groove depth of the grating.

IV. DISCUSSION

We shall calculate the reflectivity on the grating in order to explain the experimental results. Many authors have theoretically studied the reflectivity of gratings. Yamashita and Tsuji[4] proposed a simple perturbation theory for surface-plasmon-polariton resonance on a sinusoidal metal grating. We shall apply their method to the surface-phonon polariton on the grating, because it includes the essential aspect of the interaction between the photon outside the sample and the surface mode and also because it can be easily applied to the analysis of the experimental result.

First we must replace the dielectric function of the plasmon system by that of the infrared-active phonon,

$$\epsilon(\omega)=\epsilon(\infty)+[\epsilon(0)-\epsilon(\infty)]\omega_{TO}^2/(\omega_{TO}^2-\omega^2-i\Gamma\omega) , \tag{4.1}$$

where $\epsilon(0)$ and $\epsilon(\infty)$ are the static and optical dielectric constants, ω_{TO} and ω_{LO} are the (angular) frequencies of the transverse- and longitudinal-optical phonons, and Γ is the broadening factor of phonon. For GaP, we have $\epsilon(\infty)=9.09$ (Ref. 5), $\omega_{TO}=365$ cm^{-1}, $\omega_{LO}=403$ cm^{-1}, and $\Gamma=1.71$ cm^{-1}. We have directly measured ω_{TO} and ω_{LO} by Raman scattering and calculated Γ using a curve fitting of the theoretical function to the experimental reflectivity R_f. The static dielectric constant $\epsilon(0)$ is determined by the Lyddane-Sachs-Teller relation.

Second, we shall include the waves with the wave vectors k_y $[=(\omega/c)\sin\theta]$, $K_g=k_y+g$, and $K_{-g}=k_y-g$ parallel to the surface and perpendicular to the groove of the grating, of which the last one was not included in Ref. 4. In the present experiment the K_{-g} wave as well as the K_g wave will be resonant to the k_y wave. In their formulation the plane of the incidence is taken to be $x=0$. The incident wave is represented by a magnetic field:

$$B_i(y,z,t)=(B_i,0,0)e^{ik_y y}e^{ik_z z}e^{i\omega t} . \tag{4.2}$$

The wave vectors of the incident, reflected, and diffracted waves are represented by k_y, k_{-y}, K_g, and K_{-g}. The solutions of Maxwell's equations can be written approximately in the form

$$B_< = e^{ik_y y}(B_i e^{ik_z z}+B_r e^{-ik_z z}) + e^{iK_g y}B_g e^{\Gamma_g z}+e^{iK_{-g} y}B_{-g}e^{\Gamma_{-g} z} \quad \text{if } z<\xi(y) , \tag{4.3}$$

$$B_> = e^{ik_y y}B_t e^{-\gamma z} + e^{iK_q y}B_g^t e^{-\gamma_g z}+e^{iK_{-g} y}B^t_{-g}e^{-\gamma_{-g} z} \quad \text{if } z>\xi(y) , \tag{4.4}$$

where

$$K_{ng}=k_y+ng \quad (n=\pm 1) , \tag{4.5}$$

$$k_y^2+k_z^2=\omega^2/c^2 , \tag{4.6}$$

$$K_{ng}^2-\Gamma_{ng}^2=\omega^2/c^2 , \tag{4.7}$$

$$k_y^2-\gamma^2=(\omega^2/c^2)\epsilon(\omega) , \tag{4.8}$$

and

$$K_{ng}^2-\gamma_{ng}^2=(\omega^2/c^2)\epsilon(\omega) . \tag{4.9}$$

Equations (4.3)–(4.9) correspond to Eqs. (2.3)–(2.9) of Ref. 4. The magnetic fields of the reflected and diffracted waves in the air $[z<\xi(y)]$ are represented by B_r, B_g, and B_{-g}. And the magnetic fields of the transmitted and

diffracted waves in GaP [$z > \xi(y)$] are represented by B_t, B_g^t, and $B^t{}_{-g}$.

Lastly the surface of the grating can be taken as follows in the first-order perturbation theory:

$$z=\xi(y)=\xi_g e^{igy}+\xi_{-g}e^{-igy}+\xi_{2g}e^{i2gy}+\xi_{-2g}e^{-i2gy} , \tag{4.10}$$

where ξ_{lg} is given by Eq. (2.3). The inclusion of ξ_{2g} and ξ_{-2g} comes from the fact that the resonance of the K_g and K_{-g} waves will be possibly affected by ξ_{2g} and ξ_{-2g}, because they are not zero (i.e., $\Delta=0.009$).

With these modifications and the boundary conditions

$$B_< = B_> \tag{4.11}$$

and

$$\frac{\partial B_<}{\partial n}=\frac{1}{\epsilon(\omega)}\frac{\partial B_>}{\partial n} \tag{4.12}$$

with

$$\frac{\partial}{\partial n}=\left[1+\left[\frac{\partial \xi(y)}{\partial y}\right]^2\right]^{-1/2}\left[\frac{\partial}{\partial z}-\frac{\partial \xi(y)}{\partial y}\frac{\partial}{\partial y}\right] \tag{4.13}$$

at the surface $z=\xi(y)$, and using the same approximation given by Eq. (2.13) in Ref. 4,

$$e^{iK_g y}e^{-\gamma_g \xi(y)}\simeq e^{iK_g y}[1-\gamma_g\xi(y)]\simeq e^{iK_g y}-\gamma_g\xi_{-g}e^{ik_y y} \tag{4.14}$$

etc., we can obtain a set of the equations corresponding to Eqs. (2.14)–(2.17) of Ref. 4,

$$\begin{aligned}
&-B_r-\xi_{-g}\Gamma_g B_g-\xi_g\Gamma_{-g}B_{-g}\\
&\qquad +B_t-\xi_{-g}\gamma_g B_g^t-\xi_g\gamma_{-g}B^t{}_{-g}=B_i ,\\
&ik_z\xi_g B_r-B_g-\xi_{2g}\Gamma_{-g}B_{-g}-\gamma\xi_g B_t\\
&\qquad +B_g^t-\xi_{2g}\gamma_{-g}B^t{}_{-g}=ik_z\xi_g B_i ,\\
&ik_z\xi_{-g}B_r-\xi_{-2g}\Gamma_g B_g-B_{-g}-\gamma\xi_{-g}B_t-\xi_{-2g}\gamma_g B_g^t\\
&\qquad +B^t{}_{-g}=ik_z\xi_{-g}B_i ,
\end{aligned} \tag{4.15}$$

$$\begin{aligned}
&ik_z B_r+\xi_{-g}\zeta_+ B_g+\xi_g\zeta_- B_{-g}-\frac{\gamma}{\epsilon(\omega)}B_t-\frac{\xi_{-g}\eta_+}{\epsilon(\omega)}B_g^t\\
&\qquad -\frac{\xi_g\eta_-}{\epsilon(\omega)}B^t{}_{-g}=ik_z B_i ,\\
&\xi_g\zeta_+ B_r-\Gamma_g B_g-\xi_{2g}\nu B_{-g}-\frac{\xi_g\eta_+}{\epsilon(\omega)}B_t-\frac{\gamma_g}{\epsilon(\omega)}B_g^t\\
&\qquad +\frac{\xi_{2g}\mu}{\epsilon(\omega)}B^t{}_{-g}=-\xi_g\zeta_+ B_i ,\\
&\xi_{-g}\zeta_- B_r-\xi_{-2g}\nu B_g-\Gamma_{-g}B_{-g}-\frac{\xi_{-g}\eta_-}{\epsilon(\omega)}B_t+\frac{\mu\xi_{-2g}}{\epsilon(\omega)}B_g^t\\
&\qquad -\frac{\gamma_{-g}}{\epsilon(\omega)}B^t{}_{-g}=-\xi_{-g}\zeta_- B_i ,
\end{aligned}$$

where

$$\zeta_\pm=\frac{\omega^2}{c^2}-k_y K_{\pm g} , \tag{4.16}$$

$$\eta_\pm=\frac{\omega^2}{c^2}\epsilon(\omega)-k_y K_{\pm g} , \tag{4.17}$$

$$\mu=\gamma_g^2-2K_g g=K_g K_{-g}-\frac{\omega^2}{c^2}\epsilon(\omega) , \tag{4.18}$$

and

$$\nu=\Gamma_g^2-2K_g g=K_g K_{-g}-\frac{\omega^2}{c^2} . \tag{4.19}$$

Equation (4.15) can be considered to represent the interaction between the photon outside the GaP sample and the surface-phonon polariton on the grating. In fact, when the surface is flat, i.e., $\xi_{lg}=0$, Eq. (4.15) is reduced to the two independent sets of equations, one of which gives the reflection of the light (photon) on the flat surface and the other gives the dispersion relation of the surface-phonon polariton

$$c^2k_y^2/\omega^2=\epsilon(\omega)/[1+\epsilon(\omega)] , \tag{4.20}$$

where $k_y=K_{ng}$. With the grating structure on the surface, the photon outside the sample and the surface-phonon polariton are mixed, and the state of the mixed wave can be obtained by solving Eq. (4.15).

The reflectivity spectrum of the p-polarized light on the grating is directly obtained by numerically solving the 6×6 matrix equation given by Eq. (4.15). The reflectivity R_p of the p-polarized component is given by $|B_r|^2/|B_i|^2$. The reflectivity R_s of the s-polarized component on the grating is equal to that on the flat surface, because it does not interact with the surface-phonon polariton, even if there exists a grating structure. The incident light is unpolarized, and then the reflectivity on the grating is given by

$$R_g=\tfrac{1}{2}R_p+\tfrac{1}{2}R_s . \tag{4.21}$$

We obtained the calculated difference R_g-R_f for the conditions of $h=0.2$, 0.8, and 1.2 μm, which are shown by the thin solid curves in Fig. 3.

The small dip in the calculated R_g-R_f spectrum is a superposition of small dips at the frequencies of the surface-phonon polaritons with K_g and K_{-g}, i.e., it appears at the frequency where the resonance condition is satisfied between the photon outside the sample and the surface-phonon polariton on the grating. The calculated reflectivity dip shows the same frequency and the same half width with the experimental spectrum. In Fig. 4, we show the calculated results of $|B_r|/|B_i|$, $|B_g|/|B_i|$, $|B_{-g}|/|B_i|$, $|B_t|/|B_i|$, $|B_g^t|/|B_i|$, and $|B^t{}_{-g}|/|B_i|$ for the sample with $h=1.2$ μm. It is clearly seen that the amplitudes of the field strengths $|B_{-g}|/|B_i|$ and $|B^t{}_{-g}|/|B_i|$ are enhanced at the frequency of the small reflectivity dip. This tells us unquestionably that the surface-phonon polaritons are strongly excited near this frequency and that the small dip comes from the mixing of the photon outside the sample with the surface-phonon polariton under the resonant condition.

On the other hand, Fig. 3 shows that the amplitude of

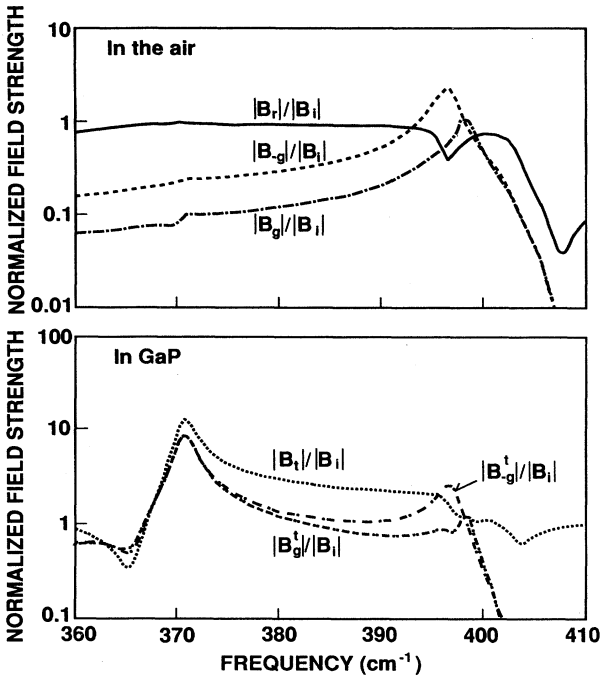

FIG. 4. The normalized magnetic field strengths of the surface-phonon polariton on the grating with the groove depth of 1.2 μm, derived from solving Eq. (4.15).

the calculated dip is about 4 times as much as the experimental dip in the case of deep groove depths $h=0.8$ and 1.2 μm. The attenuation coefficients of the resonant surface-phonon polariton with K_{-g} are represented by Γ_{-g} in the air and γ_{-g} in GaP. In the present experiment, the attenuation depths Γ_{-g}^{-1} and γ_{-g}^{-1} can be estimated from Eqs. (4.7) and (4.9) using Eq. (4.1), and they reach approximately 2 and 4 μm, respectively, at 396.5 cm^{-1}, where the reflectivity dip is observed. In the samples with $h=0.8$ and 1.2 μm, the attenuation depths are of the same order of h, and the surface-phonon-polariton field is seriously affected by the periodic structure of the surface. Then the applicability of the first-order perturbation becomes worse, and we cannot compare the experimental result with the calculated result quantitatively. This, we think, is the reason why the experimental result in the sample with $h=0.2$ μm can be well fitted to the theory, but those in the samples with larger h can be only qualitatively explained by the theory. Thus we have confirmed that the reflectivity dip originates from the mixing of the surface-phonon polariton with the photon outside the sample on the grating surface.

We have already seen that the experimental reflectivity increases near the frequency of the TO phonon on the grating surface. The difference $R_g - R_f$ of the experimental reflectivities between the sample with the grating and the flat sample has a small hump near the frequency of the TO phonon as shown in Fig. 3. The experimental hump height depends on the groove depth. The calculated difference spectra shown in Fig. 3 have also a small hump near the frequency of the TO phonon. It moves to higher frequency as the grating groove becomes deeper. The height of the hump also depends on the groove depth. Although the calculated half-width and frequency of the hump are different from the experimental results, the appearance of the hump and its behavior are qualitatively interpreted by the calculation. Then, we can see that the hump also comes from the interaction of the photon outside the sample and the surface-phonon polariton due to the existence of the grating. In contrast with the case of the reflectivity dip, which occurs owing to the resonance of the surface-phonon polariton with the photon outside the sample, we cannot easily understand what types of microscopic processes brings about the reflectivity hump. In fact, the photon outside the sample cannot resonate to the surface-phonon polariton near the frequency of the TO phonon, because the dispersion relation of the photon outside the sample does not cross that of the surface-phonon polariton even if we take into account the "folding" of the dispersion relation due to the grating. This prevents us from the clear explanation of the reflectivity hump. We can, however, explain the origin of the hump as follows.

The present formulation includes the process that the surface-phonon polariton excited by the incident photon is backscattered to the reflected photon.[4] This process causes the radiation damping of the surface-phonon polariton. The radiation damping of the surface-phonon polariton has a maximum at the frequency of the TO phonon in the case of the flat surface, because the imaginary part of the dielectric function given by Eq. (4.1) diverges near the frequency of the TO phonon.[5] In Fig. 4, the calculated magnitudes $|B_t|/|B_i|$, $|B_g^t|/|B_i|$, and $|B^t{}_{-g}|/|B_i|$ have maxima at the frequency of the small reflectivity hump. This fact suggests that the field strength of the surface phonon polariton in GaP reaches a maximum value, i.e., the surface-phonon polaritons are strongly excited possibly owing to the divergent nature of the dielectric function but not owing to the resonance due to the "folding."

The excitation of the surface-phonon polaritons does not necessarily mean the decrease of the reflectivity. Its excitation and the dissipation of its energy may induce the decrease of the reflectivity, as was observed at the reflectivity dip near 396.5 cm^{-1}. But the backscattering process via the excitation of the surface-phonon polariton, which is implicitly included in Eq. (4.15), can induce the increase of the reflectivity under some limited circumstances. The condition for the increase of the reflectivity is that the energy dissipation through the backscattering process via the excitation of the surface-phonon polariton is less than that of the usual reflection process on the flat surface. As we can see from Fig. 4, a weak hump of calculated reflectivity of the grating surface near the TO phonon is evidently accompanied by the increase of the field strength of the surface-phonon polariton. This fact unquestionably means that the energy dissipation is really reduced by the occurrence of the backscattering via the excitation of the surface-phonon polariton. Therefore, we conclude that the backscattering process via the creation of the surface-phonon polariton gives rise to the hump of the reflectivity near the frequen-

cy of the TO phonon, where the divergent nature of the dielectric function strongly contributes to the excitation of the surface-phonon polariton.

V. CONCLUSION

The surface-phonon polariton on the gratings has been investigated by far-infrared-reflectivity measurement without using an ATR prism. Reflectivity spectra show a small dip at the frequency of the surface-phonon polariton whose wave vector parallel to the surface is equal to that of the incident photon plus or minus the reciprocal lattice vector of the grating, i.e., it comes from the resonance effect between the surface-phonon polariton and the photon outside the sample, whose coupling is induced by the formation of the grating on the surface and the accompanying "folding" of the dispersion relation. The experimental results were analyzed by extending the improved perturbation theory of Yamashita and Tsuji originally applied to the surface plasmon polariton on a metal grating. The agreement between the experimental results and the theory confirms this interpretation, although the agreement was only qualitative when the depth of the grating is large. In addition, a new feature of the reflectivity spectra was discovered. A small hump was observed in the reflectivity spectra near the frequency of the transverse-optical phonon with the formation of the grating. The experimental results clearly show that the hump also comes from the mixing of the surface-phonon polariton and the photon outside the sample. But at this frequency the resonance effect cannot occur. By using the calculation based on the perturbation, we interpreted this phenomenon by the backscattering process via the creation of the surface-phonon polariton, which is associated with the divergent nature of the dielectric function near this frequency.

ACKNOWLEDGMENTS

We would like to thank Dr. K. Yanagida of Fujitsu Limited, Dr. M. Mihara of Optoelectronics Joint Research Laboratory, T. Yoshida, Professor K. Shohno, and Professor K. Ishikawa of Sophia University for their collaboration on the production of the GaP gratings.

---

*Present address: Display Devices Laboratory, Fujitsu Laboratories Ltd. Atsugi, 10-1 Morinosato-Wakamiya, Atsugi 243-01, Japan.

[1]E. A. Vinogradov, G. N. Zhizhin, and V. I. Yudson, in *Surface Polaritons,* edited by V. M. Agranovich and D. L. Mills (North-Holland, Amsterdam, 1982), p. 145.

[2]T. Sekine, J. Watanabe, K. Uchinokura, and E. Matsuura, in *Proceedings of the 2nd International Conference on Phonon Physics, Budapest, 1985,* edited by J. Kollár, N. Kroó, N. Manyhárd, and T. Sikros (World Scientific, Singapore, 1985), p. 735.

[3]F. Toigo, A. Marvin, V. Celli, and N. R. Hill, Phys. Rev. B **15**, 5618 (1976).

[4]M. Yamashita and M. Tsuji, J. Phys. Soc. Jpn. **52**, 2462 (1983).

[5]J. S. Nkoma and R. Loudon, J. Phys. C **8**, 1950 (1975).